

Suppression of local heat flux in a turbulent magnetized intracluster medium

S. V. Komarov^{1,2,3}, E. M. Churazov^{1,2} and A. A. Schekochihin⁴

¹*Max Planck Institute for Astrophysics, Karl-Schwarzschild-Strasse 1, 85741 Garching, Germany*

²*Space Research Institute (IKI), Profsovnaya 84/32, Moscow 117997, Russia*

³*Moscow Institute of Physics and Technology (MIPT), Institutskiy pereulok 9, Dolgoprudny 141700, Moscow Region, Russia*

⁴*The Rudolf Peierls Centre for Theoretical Physics, University of Oxford, 1 Keble Road, Oxford OX1 3NP, United Kingdom*

6 April 2013

ABSTRACT

X-ray observations of hot gas in galaxy clusters often show steeper temperature gradients across cold fronts – contact discontinuities, driven by the differential gas motions. These sharp (few kpc wide) surface brightness/temperature discontinuities would be quickly smeared out by the electron thermal conduction in unmagnetized plasma, suggesting significant suppression of the heat flow across the discontinuities. In fact, the character of the gas flow near cold fronts is favorable for suppression of conduction by aligning magnetic field lines along the discontinuities. We argue that a similar mechanism is operating in the bulk of the gas. Generic 3D random isotropic and incompressible motions increase the temperature gradients (in some places) and at the same time suppress the conduction by aligning the magnetic field lines perpendicular to the temperature gradient. We show that the suppression of the effective conductivity in the bulk of the gas can be linked to the increase of the frozen magnetic field energy density. On average the rate of decay of the temperature fluctuations $d\langle\delta T^2\rangle/dt$ decreases as $\langle B^2\rangle^{-1/5}$.

Key words: key words

1 INTRODUCTION

X-ray observations of galaxy clusters reveal significant spatial fluctuations of the gas temperature in a range of spatial scales (e.g., Markevitch et al. 2003). Given a temperature map with prominent fluctuations, it is possible to calculate an upper limit on the effective thermal conductivity, provided that the lifetime of the fluctuations can be estimated. It turns out to be at least an order of magnitude lower than the Spitzer conductivity for unmagnetized plasma (Ettori & Fabian 2000; Markevitch et al. 2003).

Heat conduction in the intracluster medium (ICM) is primarily along the field lines because the Larmor radius of the particles is very small compared to the collisional mean free path (Braginskii 1965). The ICM undergoes turbulent motion in a range of spatial scales (Inogamov & Sunyaev 2003; Schuecker et al. 2004; Schekochihin & Cowley 2006; Subramanian et al. 2006; Zhuravleva et al. 2011). As the magnetic field is, to a good approximation, frozen into the ICM, the field lines become tangled by gas motions and their topology changes constantly. To study thermal conduction in such tangled magnetic fields, some authors employed the random-walk representation of the magnetic field lines (Tribble 1989; Malyshkin 2001). Four main effects should be con-

sidered. Firstly, parallel thermal conduction along stochastic magnetic field lines may be reduced because the heat-conducting electrons become trapped and detrapped between regions of strong magnetic field (magnetic mirrors, see Chandran & Cowley 1998; Chandran et al. 1999; Malyshkin & Kulsrud 2001; Albright et al. 2001). Secondly, diffusion in the transverse direction may be boosted due to spatial divergence of the field lines (Skilling et al. 1974; Rechester & Rosenbluth 1978; Chandran & Cowley 1998; Narayan & Medvedev 2001; Chandran & Maron 2004). Thirdly, there is effective diffusion due to temporal change in the magnetic field (“field-line wandering”). Finally, if one is interested in temperature fluctuations and their diffusion, one must be mindful of the fact that the temporal evolution of the magnetic field is correlated with the evolution of the temperature field because the field lines and the temperature are advected by the same turbulent velocity field.

In this paper, we focus on the last effect. The more conventional approach, often used to estimate the relaxation of the temperature gradients, is to consider the temperature distribution as given and study the effect of a tangled magnetic field on the heat conduction. However, the direction and value of the fluctuating temperature gradients are not statistically independent of the direction of the magnetic

field lines because the latter are also correlated with the turbulent motions of the medium. We argue that, dynamically, the fluctuating gradients tend to be oriented perpendicular to the field lines and so heat fluxes are the more heavily suppressed the stronger the thermal gradients are. We also establish the relationship between the average conductivity and the growth of the magnetic energy density.

The structure of the paper is as follows. In § 2, we provide a qualitative explanation of the correlation between the temperature gradients and the magnetic field direction, accompanied by a number of numerical examples. In § 3, a theoretical framework for modelling this effect is presented and the joint PDF of the thermal gradients, the angles between these gradients and the magnetic field lines and the magnetic-field strength is derived in the solvable case of a simple model velocity field. The connection between the effective conductivity and the increase of the magnetic energy density is established. Analytical results are supplemented by numerical calculations in § 3.4, which extrapolate our results to the case of a more general velocity field. In § 4, we provide a general discussion (including of the limitations of our treatment). Finally, in § 5, we sum up our findings.

2 QUALITATIVE DISCUSSION

We consider a volume of plasma with high electric conductivity and frozen-in magnetic field tangled on a scale much greater than the mean free path of the particles. We also assume the plasma motions to be incompressible, which is a good approximation for subsonic dynamics. Across the paper we treat the temperature as a passive scalar.

2.1 Illustrative example: conduction between converging layers of magnetised plasma

Consider two parallel layers of an incompressible medium vertically separated by distance h with temperatures $T_1 \neq T_2$. This is illustrated in Fig. 1: the direction of the field line is shown with the inclined solid line, making an angle θ with the vertical, so $\cos \theta = h/\sqrt{h^2 + l^2}$, where l is the horizontal distance between the footpoints of the field line anchored in the two layers. An incompressible flow with $\partial_y u_y < 0$ reduces h and increases l so that $l \times h$ is conserved (in the absence of tangential shear). Here we are interested in the heat exchange between the layers, i.e., only the component of the heat flux along the temperature gradient $Q_{\nabla T}$ has to be calculated:

$$Q_{\nabla T} = \chi(\mathbf{b} \cdot \nabla T) \cos \theta = \chi \frac{T_2 - T_1}{\sqrt{h^2 + l^2}} \frac{h}{\sqrt{h^2 + l^2}}. \quad (1)$$

Let $h(t) = h_0 f(t)$ and $l(t) = l_0/f(t)$. Then

$$Q_{\nabla T} = \chi \frac{T_2 - T_1}{h_0} \frac{f}{f^2 + (l_0/h_0)^2 f^{-2}}, \quad (2)$$

where χ is the parallel thermal diffusivity coefficient (Braginskii 1965), which is assumed constant across the volume for simplicity. Therefore, in the limit of $f \rightarrow 0$, $Q_{\nabla T} \rightarrow 0$ if $l_0 \neq 0$. Similarly, when $f \rightarrow \infty$, $Q_{\nabla T} \rightarrow 0$. The decrease of the heat flux at $f > 1$ is simply due to the increase of the distance between the plates and corresponding decrease of the temperature gradient. The decrease at $f < 1$ is due to

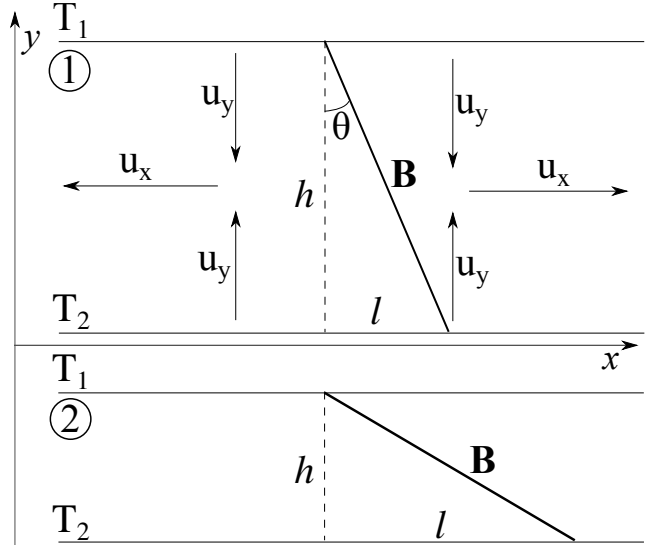


Figure 1. Correlated changes of the temperature gradients and the inclination of the magnetic field lines in the case of a converging incompressible flow: plane parallel layers at different temperatures. Converging flow with $\partial_y u_y < 0$ reduces h and increases the temperature gradient $(T_2 - T_1)/h$, but suppresses heat flux (Fig. 2). The solid line represents the direction of the magnetic field. If the medium is incompressible then $l \times h$ is conserved (in the absence of tangential shears).

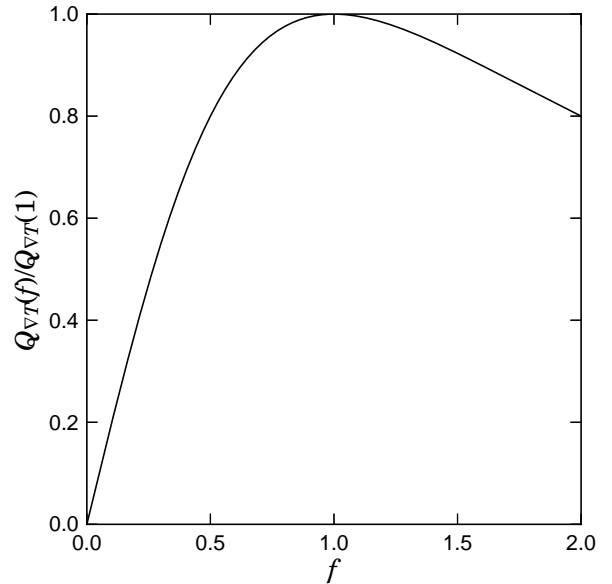


Figure 2. Suppression of the heat flux along the temperature gradient between two approaching/receding plates as a function of distance f between the plates, when the medium between the plates is threaded by tangled magnetic field [see equation (3)]. At the initial moment ($f = 1$), all angles between the magnetic field direction and the plates are equally probable. The decrease of the heat flux at $f > 1$ is simply due to the increase of the distance between the plates and corresponding decrease of the temperature gradient. The decrease at $f < 1$ is due to systematic increase of the angle between the field lines and the direction of the temperature gradient.

systematic increase of the angle between the field lines and the direction of the temperature gradient.

If at some moment the field lines are tangled in such a way that all angles θ are equally probable, then parametrizing compression/stretching along y by the same factor f and averaging over θ gives us the suppressed heat flux along the temperature gradient:

$$Q_{\nabla T} = \chi \frac{T_2 - T_1}{h_0} \frac{2f}{f^2 + 1} \quad (\text{see Fig. 2}). \quad (3)$$

Thus, increasing the temperature gradient by squeezing the layers of the gas does not boost the heat exchange between them but rather makes it smaller. A qualitatively similar situation might occur at the cold fronts – contact discontinuities formed by differential gas motions, a very simple model of which is discussed in the next subsection.

2.2 Astrophysical example: model of a cold front

Chandra observations of galaxy clusters often show sharp discontinuities in the surface brightness of the ICM emission (see review by Markevitch & Vikhlinin 2007). Most of these structures have lower-temperature gas on the brighter (higher-density) side of the discontinuity, suggesting that they are contact discontinuities rather than shocks. In the literature, these structures are called “cold fronts”. Because of the sharp temperature gradients, the limits on the thermal conduction derived for the observed cold fronts are strong (see, e.g., Ettori & Fabian 2000; Vikhlinin et al. 2001; Xiang et al. 2007).

In the majority of theoretical models, the formation of a cold front involves relative motion of cold and hot gases. Here we consider the case of a hot gas flowing around a colder, gravitationally bound gas cloud, which is a prototypical model of a cold front. For simplicity, we assume that the velocity field can be approximated with a 2D potential flow past a cylinder, while the initial temperature is symmetric around the cylinder. The initial temperature distribution and stream lines of the flow are shown in the left panel of Fig. 3. The middle panel shows the field lines of a random magnetic field superimposed on this initial temperature distribution. The evolved temperature and magnetic field are shown in the right panel of Fig. 3. Stretching of the fluid elements near the stagnation point along the front leads to the contraction of the same elements in the direction perpendicular to the front. This configuration has been considered in a number of studies of the cold fronts (see, e.g., Asai et al. 2007; Churazov & Inogamov 2004; Roediger et al. 2011). Qualitatively, it corresponds to the situation sketched in § 2.1 and Fig. 1, which naturally leads to the field lines orthogonal to the temperature gradient at the front.

2.3 Local correlation between the magnetic field strength and the heat flux

Let us now discuss the suppression of the local heat flux in more general terms. Consider the induction equation for an incompressible medium and the advection equation for the temperature:

$$\frac{d\mathbf{B}}{dt} = \mathbf{B} \cdot \nabla \mathbf{u}, \quad (4)$$

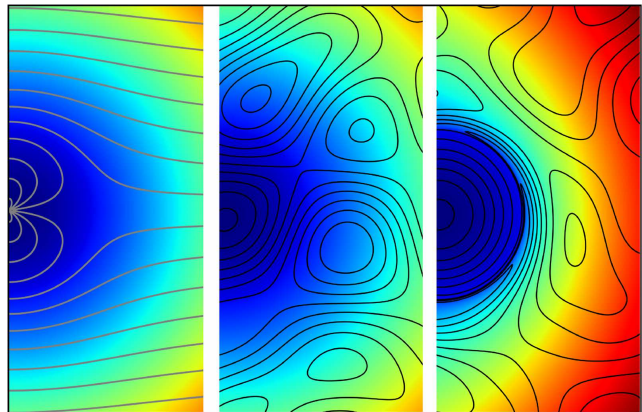


Figure 3. Alignment of the field lines perpendicular to the temperature gradient for the velocity field characteristic of a cold front. A potential flow past a cylinder is used in this example. The left panel shows the initial temperature distribution (color image) and stream lines of the velocity field. The middle panel shows a random tangled magnetic field superposed on this initial situation. The right panel shows the time-evolved temperature map and magnetic field lines (superposed contours) in such a flow. The flow boosts the temperature gradient at the cold front and at the same time stretches the field lines along the lines of constant temperature. In the resulting configuration, the field lines are essentially perpendicular to the sharp temperature gradient at the front.

$$\frac{dT}{dt} = 0, \quad (5)$$

where \mathbf{B} is the magnetic field, \mathbf{u} the velocity field, T temperature and $d/dt = \partial/\partial t + \mathbf{u} \cdot \nabla$. We have neglected thermal and magnetic diffusivities. Let \mathbf{g} be the unit vector in the direction of the temperature gradient, \mathbf{b} the unit vector in the direction of the field line, B the magnetic field magnitude and G the temperature gradient magnitude, so $\mathbf{B} = B\mathbf{b}$, $\nabla T = G\mathbf{g}$. The above equations imply:

$$\frac{dG}{dt} = -G\mathbf{g} \cdot (\nabla \mathbf{u}) \cdot \mathbf{g}, \quad (6)$$

$$\frac{dB}{dt} = B\mathbf{b} \cdot (\nabla \mathbf{u}) \cdot \mathbf{b}, \quad (7)$$

$$\frac{d\mu}{dt} = \mu[\mathbf{g} \cdot (\nabla \mathbf{u}) \cdot \mathbf{g} - \mathbf{b} \cdot (\nabla \mathbf{u}) \cdot \mathbf{b}], \quad (8)$$

where $\mu = \mathbf{b} \cdot \mathbf{g}$, the cosine of the angle between \mathbf{B} and ∇T . From these equations, we can immediately infer the following equation for $\mathbf{b} \cdot \nabla T = \mu G$, a quantity proportional to the parallel heat flux:

$$\frac{d \ln(\mu G)}{dt} = -\frac{d \ln B}{dt}. \quad (9)$$

Thus, locally, the heat flux decreases as the field strength grows.

2.4 Numerical example: a random 2D velocity field

In this example, we consider a random temperature distribution and a random magnetic field in a random δ -correlated Gaussian incompressible 2D velocity field (Fig. 4). The temperature $T(x, y)$, the magnetic field $\mathbf{B}(x, y)$ and the velocity field $\mathbf{u}(x, y)$ (assumed incompressible, $\nabla \cdot \mathbf{u} = 0$) are modeled as superpositions of Fourier harmonics with random

phases and amplitudes. The temperature and the magnetic field are advected according to equations (4) and (5). The velocity field is varied at each time step as a δ -correlated in time field. The initial conditions are shown in the top panel of Fig. 4; there is no initial correlation between the temperature gradients and the orientation of the field lines. With time, preferential stretching/squeezing of the fluid elements leads to alignment of the field lines along the isotherms (see bottom panel in Fig. 4). This happens in all regions where the stretching/squeezing is sufficiently strong. As a result, the field lines are mostly perpendicular to the direction of the temperature gradient in all regions where the gradient is large. Intuitively, one expects this tendency of local alignment between the magnetic field and the isotherms to manifest itself statistically, in a turbulent conducting medium. In the next section, we work out a simple statistical model of this process.

3 HEAT CONDUCTION IN A STOCHASTIC VELOCITY FIELD

Here we treat the suppression of the heat conduction using an analytically solvable model that allows us to predict the statistical distribution of the cosine of the angle between the thermal gradient and the field line (μ), the magnitude of the thermal gradient (G) and the magnetic-field strength (B). After the joint probability distribution function (PDF) of μ , G and B is derived (§ 3.5), we will be in a position to assess how statistically prevalent the behaviour discussed in § 2.4 is, but we will preface this detailed calculation with some simpler arguments to quantify the suppression of the heat flux.

3.1 Relaxation of temperature fluctuations

Let us restore heat conduction in equation (5):

$$\frac{dT}{dt} = \nabla \cdot (\chi \mathbf{b} \mathbf{b} \cdot \nabla T), \quad (10)$$

where χ is the parallel thermal diffusivity coefficient (Braginskii 1965). Then the volume-averaged rate of change of the rms temperature fluctuations is

$$\frac{d\langle \delta T^2 \rangle}{dt} = -2\chi \langle |\mathbf{b} \cdot \nabla \delta T|^2 \rangle = -2\chi \langle \mu^2 G^2 \rangle. \quad (11)$$

Thus, the average value of $\mu^2 G^2$ characterizes the rate at which local temperature variations are wiped out by the thermal conduction.

3.2 Kazantsev-Kraichnan model

We consider the magnetic field to be so weak that it does not affect the velocity field. This condition is only satisfied if the magnetic energy density is much lower than the kinetic energy density of the plasma motions. This means that our model does not describe the saturated state, when these energy densities become comparable. The non-saturated regime could be a common transient situation in the ICM, at least locally, in the sense that at any given time, the magnetic field is amplified up to the saturation value only in a small fraction of the volume.

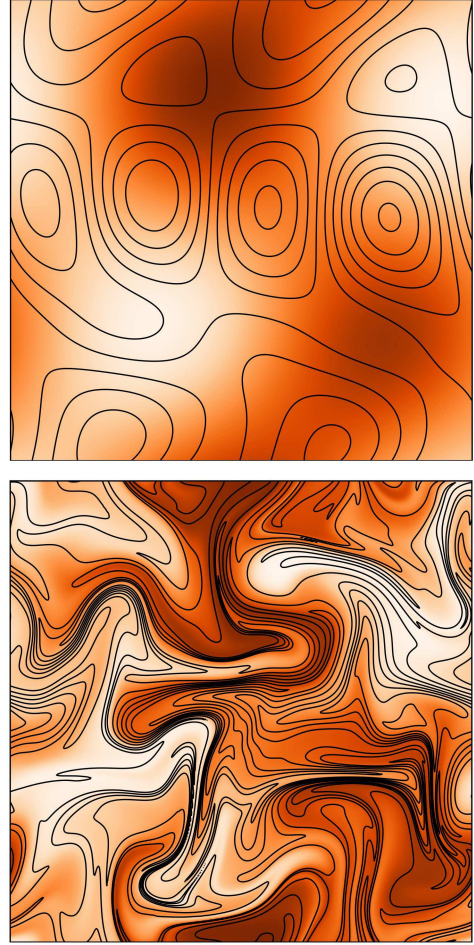


Figure 4. Alignment of the field lines perpendicular to the temperature gradient for a stochastic δ -correlated Gaussian incompressible velocity field, modeled as a superposition of Fourier harmonics with random phases and amplitudes. The top panel shows the initial random temperature distribution (color) with the field lines of a random magnetic field superposed (they are uncorrelated with temperature). The bottom panel shows the same fields later on in the evolution. In the evolved image, field lines follow the lines of constant temperature in the regions where the temperature gradient is large.

We will wish to calculate the joint PDF $p(\mu, G, B; t)$, where μ and G are defined in § 2, and investigate the evolution of the relevant correlations, viz., $\langle \mu^2 G^2 \rangle$ (see § 3.1). To do that, we need to average the dynamical equations for \mathbf{g} , \mathbf{b} , G and B over all realizations of the stochastic velocity field. The equations are:

$$\begin{aligned} \frac{dg^k}{dt} &= -(\delta_m^k - g^k g^m) g^i \partial_m u^i, \\ \frac{db^k}{dt} &= (\delta_i^k - b^k b^i) b^m \partial_m u^i, \\ \frac{dG}{dt} &= -G g^i g^m \partial_m u^i, \\ \frac{dB}{dt} &= B b^i b^m \partial_m u^i, \end{aligned} \quad (12)$$

where summation over repeated indices is implied.

This problem is solvable analytically for a Gaussian white-in-time velocity field (Kazantsev 1968):

$$\langle u^i(t, \mathbf{x}) u^j(t', \mathbf{x}') \rangle = \delta(t - t') \kappa^{ij}(\mathbf{x} - \mathbf{x}'), \quad (13)$$

where κ^{ij} is the correlation tensor, whose form can be determined from symmetry and incompressibility considerations. We may assume the medium to be isotropic and homogeneous. Consider a spatial scale much smaller than that of the stochastic velocity field. Then, at any arbitrary point, the velocity can be expanded in linear approximation:

$$u^i(t, \mathbf{x}) = \sigma_m^i(t) x^m, \quad (14)$$

where $\sigma_m^i(t) = \partial_m u^i$ and we have assumed $u^i(t, 0) = 0$ without loss of generality (otherwise change the reference frame). Then the velocity gradients satisfy

$$\left\langle \frac{\partial u^i}{\partial x^m}(t, \mathbf{x}) \frac{\partial u^j}{\partial x'^n}(t', \mathbf{x}') \right\rangle \Bigg|_{\mathbf{x}=\mathbf{x}'} = \langle \sigma_m^i(t) \sigma_n^j(t') \rangle = \delta(t - t') \kappa_{mn}^{ij}, \quad (15)$$

where

$$\kappa_{mn}^{ij} = - \frac{\partial^2 \kappa^{ij}(\mathbf{y})}{\partial y_m \partial y_n} \Bigg|_{\mathbf{y}=0} \equiv \kappa T_{mn}^{ij},$$

where $\kappa = 1/\tau_{eddy}$, τ_{eddy} is the turn-over time of the turbulent eddies and

$$T_{mn}^{ij} = \delta^{ij} \delta_{mn} - \frac{1}{d+1} \left(\delta_m^i \delta_n^j + \delta_n^i \delta_m^j \right) \quad (16)$$

is the inevitable tensor form of κ_{mn}^{ij} for an isotropic incompressible medium of dimension d ($= 2, 3$). This is the so-called Kazantsev-Kraichnan model, which has been a popular tool for modelling the properties of small-scale dynamo and passive-scalar advection in turbulent media (e.g., Chertkov et al. 1999; Balkovsky & Fouxon 1999; Boldyrev & Schekochihin 2000; Schekochihin et al. 2002, 2004; Boldyrev & Cattaneo 2004, and references therein).

3.3 Relation between magnetic field amplification and suppression of conduction for the white-in-time velocity field

Before presenting the full statistical calculation, we wish to give a relatively simple one that establishes the connection between the relaxation rate of the temperature fluctuations and the magnetic energy density. The heat flux along the field line μG is inversely proportional to the length of a field-line segment s . Therefore, one can relate the change of the mean square heat flux $\langle \mu^2 G^2 \rangle$, which is also the decay rate of the temperature fluctuations (see §3.1), to the growth of the magnetic-energy density as follows:

$$\langle B^2 \rangle \propto \langle s^2 \rangle, \quad \langle \mu^2 G^2 \rangle \propto \langle 1/s^2 \rangle. \quad (17)$$

As explained in § 3.2, we assume an isotropic linear random velocity field. Let it be piecewise constant in time over intervals τ_c and completely uncorrelated for $\Delta t > \tau_c$. Assume further that the amount of stretching of any fluid element over individual time intervals of duration $\sim \tau_c$ is small compared to the size of the element, which amounts to a model of white-noise field. Under these assumptions,

it is easy to obtain the PDF of s as a function of time t in the limit $t/\tau_c \gg 1$. The evolution of each component of the separation vector \mathbf{x} of any two locations frozen into a velocity field constant over time interval τ_c is

$$x^i(\tau_c) \approx x^i(0) + \tau_c \sigma_j^i x^j(0) + \frac{1}{2} \tau_c^2 \sigma_j^i \sigma_k^j x^k(0) + O(\tau_c^3), \quad (18)$$

where σ_j^i is the velocity gradients matrix [see equation (14)]. Since we are dealing with a random isotropic field, we can set $\mathbf{x}(0) = (1, 0, 0)$ at $t = 0$. Then

$$x^1(\tau_c) \approx 1 + \tau_c \sigma_1^1 + \frac{1}{2} \tau_c^2 \sigma_j^1 \sigma_1^j + O(\tau_c^3), \\ x^{i \neq 1}(\tau_c) = \tau_c \sigma_1^i + O(\tau_c^2). \quad (19)$$

We are interested in the time evolution of the ‘‘stretching factor’’ $s^2 = |\mathbf{x}|^2$. For one ‘‘act of stretching’’, equation (19) implies

$$\ln s^2(\tau_c) = 2\tau_c \sigma_1^1 - 2\tau_c^2 (\sigma_1^1)^2 + \tau_c^2 \sigma_1^j \sigma_1^j + \tau_c^2 \sigma_j^1 \sigma_1^j + O(\tau_c^3). \quad (20)$$

For $t \gg \tau_c$, the calculation of $s^2(t)$ reduces to summation of $N = t/\tau_c \gg 1$ such independent stretching episodes:

$$\ln s^2(t) = \sum \ln s^2(\tau_c). \quad (21)$$

After applying the central limit theorem to $(1/N) \sum \ln s^2(\tau_c)$, one readily gets the PDF of s^2 :

$$P(s^2) = \frac{1}{s^2} \frac{1}{\sqrt{2\pi\sigma_s^2}} e^{-\frac{(\ln s^2 - m_s)^2}{2\sigma_s^2}}, \quad (22)$$

where

$$\sigma_s = 2\sqrt{\frac{T_{11}^{11}}{\tau_{eddy}} \frac{t}{\tau_{eddy}}}, \\ m_s = \left[-2T_{11}^{11} + \sum_{i=1}^d \left(T_{11}^{ii} + T_{1i}^{i1} \right) \right] \frac{t}{\tau_{eddy}}, \quad (23)$$

where τ_{eddy} and T_{mn}^{ij} are defined at the end of § 3.2. We have taken $\delta(0) = 1/\tau_c$ in equation (15). Using equation (17), we get

$$\langle B^2 \rangle \propto e^{m_s + \sigma_s^2/2}, \quad \langle \mu^2 G^2 \rangle \propto e^{-m_s + \sigma_s^2/2}. \quad (24)$$

This leads to a simple relation between the growing magnetic-energy density and the evolution of the mean square heat flux:

$$\langle \mu^2 G^2 \rangle \propto \langle B^2 \rangle^p, \quad \text{where } p = \frac{-m_s + \sigma_s^2/2}{m_s + \sigma_s^2/2}. \quad (25)$$

For an incompressible velocity field in 3D, using equation (16), we get $p = -1/5$. This is a statistical version of the dynamical equation (9). It implies that on average, as the magnetic-energy density grows, the rate of decay of the temperature fluctuations is reduced, although the efficiency of this reduction is modest (p is low). This is because $\langle \mu^2 G^2 \rangle$ is dominated by regions of low stretching while $\langle B^2 \rangle$ by regions of high stretching [equation (17)] and the distribution of these is highly intermittent.

3.4 Finite-time correlated velocity field

How sensitive is this result to the obviously unphysical assumption of zero correlation time? Here, we numerically calculate the PDF of s in a random incompressible 3D velocity

field evolving according to a Langevin equation with a finite correlation time. This is a generalization of the δ -correlated case considered in § 3.3.

We consider a large number of independent field-line segments, each one placed in its own stochastic incompressible velocity field, given by equation (14), where the velocity gradient satisfies

$$\frac{d\sigma_m^i}{dt} = -\frac{1}{\tau_c}\sigma_m^i + \partial_m a^i, \quad (26)$$

where τ_c is the correlation time and the gradient of the stochastic acceleration a^i satisfies

$$\langle \partial_m a^i(t) \partial_n a^j(t') \rangle = \delta(t-t') A^2 T_{mn}^{ij}. \quad (27)$$

Here A^2 is the noise amplitude and the dimensionless tensor T_{mn}^{ij} is fixed by isotropy and incompressibility as given by equation (16). It is possible to define the effective turn-over time of turbulent eddies τ_{eddy} in much the same way as we did for the δ -correlated case:

$$\int_0^\infty \langle \sigma_m^i(0) \sigma_n^j(t) \rangle dt = \frac{1}{2} A^2 \tau_c^2 T_{mn}^{ij} \equiv \frac{1}{2\tau_{eddy}}, \quad (28)$$

where the exact solution of the Langevin equation (26) has been substituted. Thus, $\tau_{eddy} = 1/(\tau_c A)^2$.

In view of equation (17), the evolution of $\langle \mu^2 G^2 \rangle$ and $\langle B^2 \rangle$ can be easily calculated from the distribution of the segment lengths. Here we do this for a range of values of the ratio $\eta = \tau_c/\tau_{eddy}$. In § 3.3, we treated the case $\eta \rightarrow 0$ analytically, whereas for a physically sound case, $\eta \approx 1$ because typically turbulent velocities decorrelate over their eddy turn-over times and fluid elements are stretched by order-unity amounts over the same time scales. The results are shown in Fig. 5. Even though the growth/decay rates of $\langle B^2 \rangle$ and $\langle \mu^2 G^2 \rangle$ do change with correlation time, their relative behaviour appears to be invariant, viz.,

$$\langle \mu^2 G^2 \rangle \propto \langle B^2 \rangle^{-1/5}, \quad (29)$$

practically the same as for the δ -correlated regime [cf. equation (25)]

Thus, finite correlation times do not change the form of the effective conduction-magnetic-energy-density relation, only modifying the time dependence. This result gives us some confidence in the Kazantsev-Kraichan velocity as a credible modelling choice.

3.5 Statistics of the heat flux

In this section we will finally derive the full joint statistical distribution of the magnetic field and the temperature gradient and hence the detailed correlations between the heat flux, the field strength and the relative direction of the magnetic field and the temperature gradient.

For a velocity field given by equation (14), we can write equations (12) for \mathbf{g} , \mathbf{b} , G and B as follows:

$$\begin{aligned} \partial_t g^k &= -(\delta_m^k - g^k g^m) g^i \sigma_m^i, \\ \partial_t b^k &= (\delta_i^k - b^k b^i) b^m \sigma_m^i, \\ \partial_t G &= -G g^i g^m \sigma_m^i, \\ \partial_t B &= B b^i b^m \sigma_m^i. \end{aligned} \quad (30)$$

There are no advection terms here due to the homogeneity of the gas (so we can consider equation (12) at $\mathbf{x} = 0$).

The details of the derivation of the equation for the joint PDF $p(\mu, G, B; t)$ are presented in Appendix A. The result is

$$\begin{aligned} \partial_t p &= \frac{\kappa}{2(d+1)} \left[2d(1-\mu^2)(\mu \partial_\mu \mu \partial_\mu - \partial_G G \mu \partial_\mu - \partial_B B \mu \partial_\mu) \right. \\ &\quad + (d-1)(\partial_G G \partial_G G + \partial_B B \partial_B B) + 2(1-\mu^2 d) \partial_G G \partial_B B \\ &\quad + d(d+1-2d\mu^2)(2\mu \partial_\mu - \partial_G G - \partial_B B) \\ &\quad \left. + 2d^2(1-d\mu^2) \right] p, \end{aligned} \quad (31)$$

where d is the dimension of space. From now on, we only consider $d = 3$.

Multiplying both sides of equation (31) by $\mu^2 G^2$ and integrating, we find

$$\partial_t \langle \mu^2 G^2 \rangle = -\frac{\kappa}{2} \langle \mu^2 G^2 \rangle, \quad (32)$$

so the mean square heat flux decays exponentially in time. Then, recalling equation (11) for the rate of smoothing of the temperature fluctuations,

$$\frac{d\langle \delta T^2 \rangle}{dt} \propto -e^{-\kappa t/2} \rightarrow 0. \quad (33)$$

We observe that the relaxation rate of the temperature fluctuations decreases significantly on time scales of the order of the turn-over time of the turbulent eddies ($\kappa = 1/\tau_{eddy}$).

It is also possible to reproduce the relation for the mean square heat flux as a function of the magnetic energy density [equation (25)]. Multiplying equation (31) by B^2 and integrating, we obtain the evolution of the magnetic energy density:

$$\partial_t \langle B^2 \rangle = \frac{5}{2} \kappa \langle B^2 \rangle. \quad (34)$$

This result, combined with equation (32), leads to the relation established in § 3.3:

$$\langle \mu^2 G^2 \rangle = \langle B^2 \rangle^{-1/5}. \quad (35)$$

We expect that the temperature gradients and the magnetic field lines will become perpendicular to each other. Let us then first investigate the limit of $\mu \rightarrow 0$, in which equation (31) can be solved analytically. Let $x = \ln \mu$, $y = \ln G$ and $z = \ln B$. Then the joint PDF of these variables is $h(x, y, z; t) = p(\mu(x), G(y), B(z); t) e^{x+y+z}$, where the last factor is the Jacobian of the transformation of variables. Taking $\mu \rightarrow 0$ in equation (31), we find that h satisfies

$$\begin{aligned} \partial_t h &= \frac{\kappa}{4} \left[3h_{xx} + h_{yy} + h_{zz} - 3(h_{xy} + h_{xz}) + h_{yz} \right. \\ &\quad \left. + 3(2h_x - h_y - h_z) \right]. \end{aligned} \quad (36)$$

Let us now write h in the following form:

$$h(x, y, z; t) = f(x, y; t) \delta(x + y + z). \quad (37)$$

Substituting this ansatz into equation (36), we find that the factorization goes through and f satisfies

$$\partial_t f = \frac{\kappa}{4} \left[3f_{xx} + f_{yy} - 3f_{xy} + 3(2f_x - f_y) \right]. \quad (38)$$

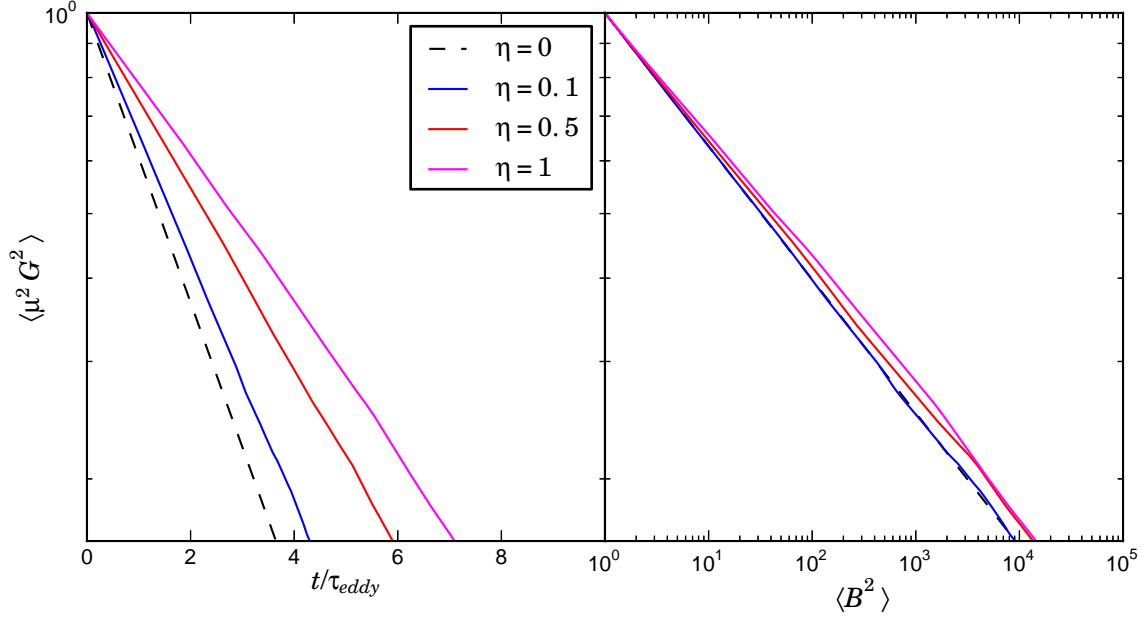


Figure 5. The decrease of the mean square heat flux $\langle \mu^2 G^2 \rangle$ for the time-correlated velocity field and different ratios $\eta = \tau_c / \tau_{eddy}$ (numerical results). While growth/decay rates of $\langle B^2 \rangle$ and $\langle \mu^2 G^2 \rangle$ change with correlation time, their relative behaviour is practically the same: $\langle \mu^2 G^2 \rangle \propto \langle B^2 \rangle^{-0.2}$.

This factorization implies that in the limit $\mu \rightarrow 0$, $\mu G \propto 1/B$ independently from the initial conditions. This result was anticipated in § 3.3, where we took the ratio of μG and $1/B$ to be the same for all the segments of the field lines at the initial moment.

Let us make another transformation: $\xi = x = \ln \mu$ and $\eta = x + 2y = \ln(\mu G^2)$ to separate variables in equation (38). The joint PDF of these two variables, $w(\xi, \eta; t) = f(x(\xi), y(\xi, \eta); t)$, satisfies

$$\partial_t w = \frac{\kappa}{4} \left(3w_{\xi\xi} + w_{\eta\eta} + 6w_{\xi} \right). \quad (39)$$

This equation can be readily solved:

$$w(\xi, \eta; t) = \frac{1}{\sqrt{3\pi\kappa t}} \int_{-\infty}^{+\infty} d\xi' d\eta' f(\xi', \eta'; 0) e^{-\frac{1}{3\kappa t} [\frac{3}{2}\kappa t + (\xi - \xi')]^2} \times e^{-\frac{1}{\kappa t} (\eta - \eta')^2}. \quad (40)$$

Notice that along with diffusion in both variables, the PDF drifts to $\xi \rightarrow -\infty$, i.e., to smaller μ . So there is a continued tendency towards mutually perpendicular orientation of the thermal gradients and the field lines.

If one is interested how the joint PDF of μ and G behaves in the case of μ order unity, full equation (31) integrated over the magnetic field strength has to be solved. Technically speaking, we are obliged to do this in order to ascertain that the limit $\mu \rightarrow 0$ was the relevant one to consider, i.e., that the joint distribution of μ and G moves towards smaller μ independently of initial conditions. Again, to separate variables, we employ the variables $\xi = \ln \mu$ and $\eta = \ln(\mu G^2)$. The PDF of these variables,

$w(\xi, \eta; t) = \int p(\mu(\xi), G(\xi, \mu), B; t) e^{\frac{1}{2}(\xi + \eta)} dB$, satisfies

$$\partial_t w = \frac{\kappa}{4} \left[3(1 - e^{2\xi})w_{\xi\xi} + (1 + 3e^{2\xi})w_{\eta\eta} + 6(1 - 2e^{2\xi})w_{\xi} - 12e^{2\xi}w \right]. \quad (41)$$

In order to solve this equation numerically, it is convenient to rewrite it in the divergence form as follows:

$$\partial_t w = \frac{\kappa}{4} \left\{ \partial_{\xi} [2(1 - e^{2\xi}) + (1 - e^{2\xi})\partial_{\xi}] + \partial_{\eta} (1 + 3e^{2\xi})\partial_{\eta} \right\} w. \quad (42)$$

Numerical solution of this equation is presented in Fig. 6. With time, the maximum of the PDF does indeed shift towards smaller μ , demonstrating that the temperature gradient and the magnetic field vector are becoming ever more orthogonal to each other. One can replot this graph in coordinates μG (heat flux) and G to observe that the rate of smearing of the temperature fluctuations in equation (11) is correlated with the magnitude of the temperature gradients (Fig. 7) in such a way that sharper gradients on average tend to be wiped out slower due to smaller corresponding values of μG .

4 DISCUSSION

We now briefly discuss the assumptions made in our model and its implications.

1) The ordering of scales in the problem considered in this paper obeys the following relations:

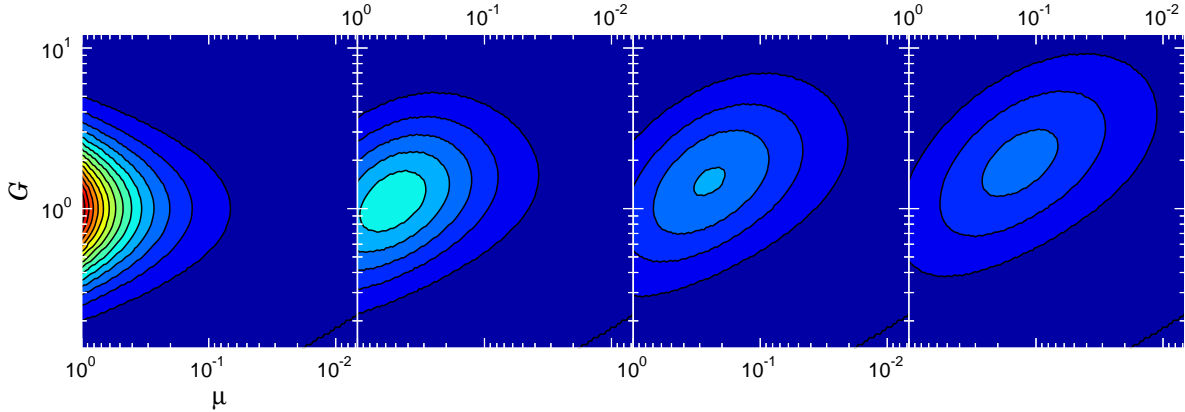


Figure 6. Evolution of the joint PDF of μ and G at regular time intervals from $t = 0$ to $t = \tau_{eddy}$ (turn-over time of the turbulent eddies) obtained via numerical solution of the equation (42). The maximum of the function drifts to the region where the thermal gradients and the field lines are perpendicular ($\mu \rightarrow 0$).

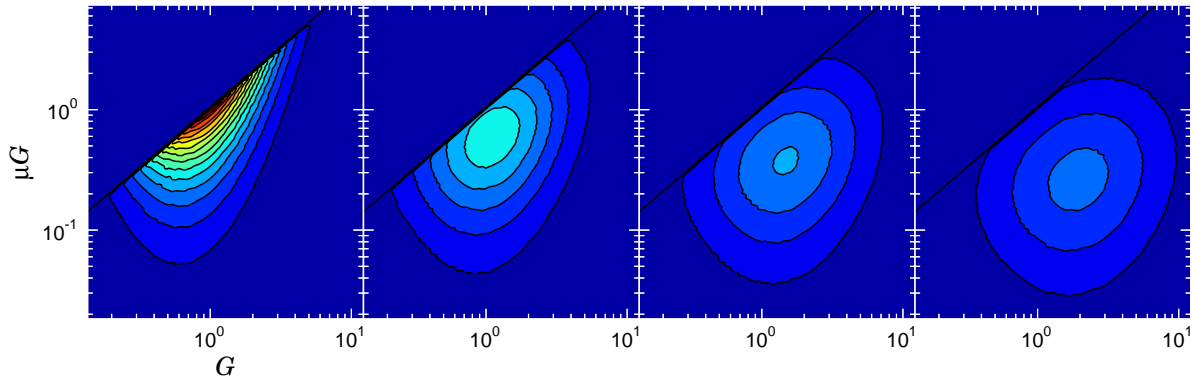


Figure 7. Evolution of the joint PDF in terms of heat flux $\mu G = |\mathbf{b} \cdot \nabla T|$ and $G = |\nabla T|$ at the same times as in Fig. 6. Sharper gradients tend to be wiped out slower due to the smaller corresponding values of the heat flux.

$$\rho_e \ll \lambda_{mfp} \lesssim l \lesssim \lambda_u, \quad (43)$$

where l is the characteristic size of the region we deal with, ρ_e is the electron Larmor radius, λ_{mfp} is the electron mean free path and λ_u is the typical size of a turbulent eddy.

The limit $l \ll \lambda_u$ simplifies the calculation of the field-line stretching because the linear expansion of the velocity field can be used [equation (14)]. This allows for analytic treatment of the problem. Note that kinematic dynamo naturally sets the parallel correlation length of the magnetic field $\lambda_{B\parallel}$ to be $\sim \lambda_u$ (Schekochihin et al. 2002, 2004).

The condition $\lambda_{mfp} \lesssim l$ allows us to apply the thermal conduction equation (10) at these spatial scales. Due to the fact that in the kinematic-dynamo regime, $\lambda_u \sim \lambda_{B\parallel}$, we also have $\lambda_{mfp} \lesssim \lambda_{B\parallel}$. This limit being assumed, we can ignore the magnetic mirroring effects because the electrons are free to escape magnetic traps by changing their pitch angles by collisions (Chandran & Cowley 1998; Chandran et al. 1999).

A typical value of $\lambda_{mfp} \sim 20 \text{ kpc} (T/10^8 \text{ K})^2 (n_e/10^{-3} \text{ cm}^{-3})^{-1}$ due to Coulomb collisions varies in the cluster cores from 0.01 to 20 kpc depending on temperature and density. For example, in the core of the Coma cluster the mean free path is ~ 5 kpc (Churazov et al. 2012); in M87/Virgo it is much smaller, viz., $\lambda_{mfp} \sim 0.01$ kpc, due to lower temperature and higher density (Churazov et al. 2008). On the other

hand, the value of λ_u can be in the range of 10 kpc to 200 kpc (Inogamov & Sunyaev 2003; Schuecker et al. 2004; Schekochihin & Cowley 2006; Subramanian et al. 2006; Zhuravleva et al. 2011; Kunz et al. 2011). Therefore, our analysis is relevant for scales between ~ 0.1 to ~ 100 kpc. Some of these scales are directly resolvable with Chandra or XMM-Newton, suggesting that the observed substructures in the temperature maps should have the magnetic field lines roughly aligned with the iso-temperature contours.

2) The assumption of incompressibility (needed to use equation (16) for the description of the velocity field) is valid as long as the gas velocities are subsonic. This is reasonable for the ICM, except for cases of strong mergers or AGN-driven strong shocks in the very core of a cluster. The comparison of cluster mass estimates from X-ray data and lensing or stellar kinematics (e.g., Churazov et al. 2008) and simulations (e.g., Lau et al. 2009) suggest that the kinetic energy of the gas motions is at the level of 5-15% of its thermal energy in the relaxed clusters. Slight deviations from incompressibility should not dramatically alter our results.

3) As shown in § 3.3, the evolution of the decay rate of the small-scale ($l \lesssim \lambda_u$) temperature variations can be linked to the amount of stretching of the field lines as $\propto \langle 1/s^2 \rangle$. Essentially the decay rate goes down because the field lines,

along which the heat is transported, are stretched¹ The amount of stretching is of course limited by saturation of the magnetic field. We note that saturation, which can be one of the key effects in the problem, is completely neglected in our paper and is a matter of further study. Another potentially important effect we have blatantly disregarded is reconnection of the field lines that constantly modifies their topology. While we believe the simple model considered in this paper correctly captures the qualitative picture, direct numerical simulations are required to confirm this.

4) We stress again that we only consider the suppression of local thermal conductivity on scales $l \lesssim \lambda_u$. We have established that the fluctuating temperature gradients are predominantly oriented perpendicular to the magnetic field lines, which slows down thermal conduction. This process resembles the one that occurs macroscopically in cold fronts where the field lines are aligned along the cold front interface by the plasma flow. If one is interested in the global heat transport on scales $l \gg \lambda_u$, other effects start to be important. In particular, the exponential divergence of the field lines and transverse diffusion of electrons increase the global conductivity (Rechester & Rosenbluth 1978; Chandran & Cowley 1998; Narayan & Medvedev 2001; Chandran & Maron 2004).

5 CONCLUSIONS

We have studied the correlations between the local fluctuating temperature gradients and the orientation of the frozen-in magnetic field lines in the turbulent ICM. One of the frequently made assumptions is that the magnetic field is randomly oriented with respect to the temperature gradients. We argue, instead, that strong correlation between the direction of the field and the temperature gradients can be expected in a turbulent ICM. Gas motions tend to increase the temperature gradients and, at the same time, align the magnetic field lines perpendicular to the gradients. Cold fronts in clusters provide a vivid example of this process at large scales. The net result of the correlated evolution of the temperature distribution and the magnetic field is the effective suppression of the local heat flux. We have calculated explicitly the joint distribution function of the gradients and the angles they make relative to the field lines and demonstrated that significant suppression takes place for generic 3D isotropic incompressible motions. The main results of this study can be summarized as follows:

- Strong correlation of the fluctuating temperature gradients and the local magnetic field orientation is established on the eddy turnaround time.
- For disturbed clusters, where large-scale clumps of gas are displaced, the largest observed gradients should be associated with the largest heat flux suppression. The estimates of the effective conductivity based on these gradients may not be characteristic of the bulk of the gas.

¹ The effect of the field-line stretching on the suppression of thermal conduction has previously been studied by Rosner & Tucker 1989 and Tao 1995, but in the case of $\lambda_B < \lambda_{mfp}$ and constant macroscopic thermal gradient.

- On average, the decay time of temperature fluctuations is anti-correlated with the amplification of the magnetic field by the gas motions. Volume averaged decay rate decreases with the growth of the magnetic energy density as $\langle B^2 \rangle^{-1/5}$. In other words, mixing of the ICM by the isotropic incompressible motions does not promote heat exchange as long as the magnetic field remains frozen.

ACKNOWLEDGMENTS

This work was supported in part by the Leverhulme Trust Network on Magnetized Plasma Turbulence.

REFERENCES

- Albright B. J., Chandran B. D. G., Cowley S. C., Loh M., 2001, *Phys. Plasmas*, 8, 777
- Asai N., Fukuda N., Matsumoto R., 2007, *ApJ*, 663, 816
- Balkovsky E., Fouxon A., 1999, *Phys. Rev. E*, 60, 4164
- Boldyrev S., Cattaneo F., 2004, *Phys. Rev. Lett.*, 92, 144501
- Boldyrev S. A., Schekochihin A. A., 2000, *Phys. Rev. E*, 62, 545
- Braginskii S. I., 1965, *Rev. Plasma Phys.*, 1, 205
- Chandran B. D. G., Cowley S. C., 1998, *Phys. Rev. Lett.*, 80, 3077
- Chandran B. D. G., Cowley S. C., Ivanushkina M., Sydora R., 1999, *ApJ*, 525, 638
- Chandran B. D. G., Maron J. L., 2004, *ApJ*, 602, 170
- Chertkov M., Falkovich G., Kolokolov I., Vergassola M., 1999, *Phys. Rev. Lett.*, 83, 4065
- Churazov E., Forman W., Vikhlinin A., Tremaine S., Gerhard O., Jones C., 2008, *MNRAS*, 388, 1062
- Churazov E., Inogamov N., 2004, *MNRAS*, 350, L52
- Churazov E., Vikhlinin A., Zhuravleva I., Schekochihin A., Parrish I., Sunyaev R., Forman W., Böhringer H., Randall S., 2012, *MNRAS*, 421, 1123
- Ettori S., Fabian A. C., 2000, *MNRAS*, 317, L57
- Furutsu K., 1963, *J. Res. NBS*, 67D, 303
- Inogamov N. A., Sunyaev R. A., 2003, *Astron. Lett.*, 29, 791
- Kazantsev A. P., 1968, *Soviet Phys. JETP*, 26, 1031
- Kunz M. W., Schekochihin A. A., Cowley S. C., Binney J. J., Sanders J. S., 2011, *MNRAS*, 410, 2446
- Lau E. T., Kravtsov A. V., Nagai D., 2009, *ApJ*, 705, 1129
- Malyshev L., 2001, *ApJ*, 554, 561
- Malyshev L., Kulsrud R., 2001, *ApJ*, 549, 402
- Markevitch M., Mazzotta P., Vikhlinin A., Burke D., Butt Y., David L., Donnelly H., Forman W. R., Harris D., Kim D.-W., Virani S., Vrtilik J., 2003, *ApJ*, 586, L19
- Markevitch M., Vikhlinin A., 2007, *Phys. Rep.*, 443, 1
- Narayan R., Medvedev M. V., 2001, *ApJ*, 562, L129
- Novikov E., 1965, *Soviet Phys. JETP*, 20, 1290
- Rechester A. B., Rosenbluth M. N., 1978, *Phys. Rev. Lett.*, 40, 38
- Roediger E., Brüggem M., Simionescu A., Böhringer H., Churazov E., Forman W. R., 2011, *MNRAS*, 413, 2057
- Rosner R., Tucker W. H., 1989, *ApJ*, 338, 761
- Schekochihin A., Cowley S., Maron J., Malyshev L., 2002, *Phys. Rev. E*, 65, 016305

- Schekochihin A. A., Cowley S. C., 2006, *Phys. Plasmas*, 13, 056501
- Schekochihin A. A., Cowley S. C., Taylor S. F., Maron J. L., McWilliams J. C., 2004, *ApJ*, 612, 276
- Schekochihin A. A., Haynes P. H., Cowley S. C., 2004, *Phys. Rev. E*, 70, 046304
- Schuecker P., Finoguenov A., Miniati F., Böhringer H., Briel U. G., 2004, *A&A*, 426, 387
- Skilling J., McIvor I., Holmes J. A., 1974, *MNRAS*, 167, 87P
- Subramanian K., Shukurov A., Haugen N. E. L., 2006, *MNRAS*, 366, 1437
- Tao L., 1995, *MNRAS*, 275, 965
- Tribble P. C., 1989, *MNRAS*, 238, 1247
- Vikhlinin A., Markevitch M., Murray S. S., 2001, *ApJ*, 549, L47
- Xiang F., Churazov E., Dolag K., Springel V., Vikhlinin A., 2007, *MNRAS*, 379, 1325
- Zhuravleva I. V., Churazov E. M., Sazonov S. Y., Sunyaev R. A., Dolag K., 2011, *Astron. Lett.*, 37, 141

APPENDIX A: STATISTICAL CALCULATION OF THE JOINT PDF OF μ , G AND B

The general form of the joint PDF of the magnetic field and the temperature gradient is

$$P(\mathbf{g}, \mathbf{b}, G, B; t) = \langle \tilde{P} \rangle, \\ \tilde{P} = \delta(\mathbf{g} - \mathbf{g}(t))\delta(\mathbf{b} - \mathbf{b}(t))\delta(G - G(t))\delta(B - B(t)), \quad (\text{A1})$$

where \mathbf{g} , \mathbf{b} , G and B are variables and $\mathbf{g}(t)$, $\mathbf{b}(t)$, $G(t)$ and $B(t)$ are stochastic processes that are solutions of equations (30). Taking time derivative of \tilde{P} and using equations (30), we obtain

$$\partial_t P = \hat{L}_i^m \sigma_m^i \tilde{P}, \quad (\text{A2})$$

where

$$\hat{L}_i^m = \frac{\partial}{\partial g^k} (\delta_m^k - g^k g^m) g^i - \frac{\partial}{\partial b^k} (\delta_i^k - b^k b^i) b^m \\ + \frac{\partial}{\partial G} g^i g^m G - \frac{\partial}{\partial B} b^i b^m B. \quad (\text{A3})$$

The average of equation (A2) is

$$\partial_t P = \hat{L}_i^m \langle \sigma_m^i \tilde{P} \rangle \quad (\text{A4})$$

and we now apply the Furutsu-Novikov formula (Furutsu 1963; Novikov 1965) to calculate the right-hand side:

$$\langle \sigma_m^i(t) \tilde{P}(t) \rangle = \int dt' \langle \sigma_m^i(t) \sigma_n^j(t') \rangle \left\langle \frac{\delta \tilde{P}(t)}{\delta \sigma_n^j(t')} \right\rangle \\ = \kappa T_{mn}^{ij} \left\langle \frac{\delta \tilde{P}(t)}{\delta \sigma_n^j(t)} \right\rangle \quad (\text{A5})$$

where we have used equation (15). From equation (A2),

$$\frac{\delta \tilde{P}(t)}{\delta \sigma_n^j(t)} = \int_{-\infty}^t dt' \left[\hat{L}_i^m \delta_j^i \delta_m^n \delta(t-t') \tilde{P}(t') \right. \\ \left. + \hat{L}_i^m \sigma_m^i(t') \frac{\delta \tilde{P}(t')}{\delta \sigma_n^j(t')} \right] = \frac{1}{2} \hat{L}_j^n \tilde{P}(t). \quad (\text{A6})$$

The second term inside the integral vanishes by causality ($t' < t$). Using equation (A6) in equation (A5) and substituting into equation (A4), we arrive at a closed equation for the desired PDF:

$$\partial_t P = \frac{\kappa}{2} T_{mn}^{ij} \hat{L}_i^m \hat{L}_j^n P. \quad (\text{A7})$$

Since the medium is isotropic, the PDF only depends on G , B and the angle between the unit vectors \mathbf{g} and \mathbf{b} . Therefore, it can be factorized as

$$P(\mathbf{g}, \mathbf{b}, G, B; t) = \frac{1}{8\pi^2} \delta(\mathbf{g}^2 - 1) \delta(\mathbf{b}^2 - 1) p(\mu, G, B; t), \quad (\text{A8})$$

where $\mu = \mathbf{b} \cdot \mathbf{g}$. The factor $1/8\pi^2$ has been introduced in order to keep $p(\mu, G, B; t)$ normalized to unity. Substituting this expression into equation (A7), we get

$$\hat{L}_i^m \hat{L}_j^n P = \delta(\mathbf{g}^2 - 1) \delta(\mathbf{b}^2 - 1) \\ \times \{ (b^i b^j b^m b^n + g^i g^j g^m g^n - g^i b^j g^m b^n \\ - b^i g^j b^m g^n) \mu \partial_\mu \mu \partial_\mu \\ + (b^i g^j b^m g^n - g^i g^j g^m g^n) \mu \partial_\mu \partial_G G \\ + (g^i b^j g^m b^n - 2b^i b^j b^m b^n + b^i g^j b^m g^n) \mu \partial_\mu \partial_B B \\ - (g^i b^j g^m b^n + b^i g^j b^m g^n) \partial_G G \partial_B B \\ + g^i g^j g^m g^n \partial_G G \partial_G G \\ + [2(d+1)(b^i b^j b^m b^n + g^i g^j g^m g^n) \\ - 2d(g^i b^j g^m b^n + b^i g^j b^m g^n) - b^m b^n \delta_j^i - b^j b^m \delta_n^i \\ - g^i g^n \delta_m^j - g^i g^j \delta_n^m] \mu \partial_\mu \\ + [-2(d+1)g^i g^j g^m g^n + d(g^i b^j g^m b^n + b^i g^j b^m g^n) \\ + g^i g^n \delta_m^j + g^i g^j \delta_n^m] \partial_G G \\ + [-2(d+1)b^i b^j b^m b^n + d g^i b^j g^m b^n + d b^i g^j b^m g^n \\ + b^m b^n \delta_j^i + b^j b^m \delta_n^i] \partial_B B \\ + d[(d+2)(b^i b^j b^m b^n + g^i g^j g^m g^n) - d(g^i b^j g^m b^n \\ + b^i g^j b^m g^n) \\ - (b^m b^n \delta_j^i + b^j b^m \delta_n^i + g^i g^n \delta_m^j + g^i g^j \delta_n^m)] \} p, \quad (\text{A9})$$

where d is the number of spatial dimensions. The PDF is factorized, as it ought to be, and we only need to solve the equation for $p(\mu, G, B; t)$. Substituting equation (A9) into equation (A7), we perform the convolutions involving T_{mn}^{ij} [see equation (16)] using the identities

$$T_{mn}^{ij} b^i b^j b^m b^n = \frac{d-1}{d+1}, \\ T_{mn}^{ij} g^i b^j g^m b^n = \frac{\mu^2 - 1}{d+1}, \\ T_{mn}^{ij} b^j b^m \delta_n^i = 0, \\ T_{mn}^{ij} b^m b^n \delta_j^i = \frac{(d-1)(d+2)}{d+1}, \\ T_{mn}^{ij} b^i g^j b^m g^n = \frac{\mu^2 - 1}{d+1}, \\ T_{mn}^{ij} g^i g^j g^m g^n = \frac{d-1}{d+1}, \\ T_{mn}^{ij} g^i g^n \delta_m^j = 0, \\ T_{mn}^{ij} g^i g^j \delta_n^m = \frac{(d-1)(d-2)}{d+1}. \quad (\text{A10})$$

The result is equation (31).